Ionic Conductivity Properties in Bismuth Germanate Silicate Glasses at Various Temperatures

Y. S. Yang,* J. H. Cho, S. J. Kim, J. E. Kim, H. W. Choi, and Young-Hoon Rim†

School of Nano Science and Technology, RCDAMP, Department of Physics, Pusan National University, Pusan 609-735, South Korea, and School of Liberal Arts, Semyung University, Chechon, Chungbuk 390-711, South Korea

Received: March 15, 2004; In Final Form: July 7, 2004

Ionic conductivities in the bismuth germanate silicate (BGSO) glasses have been investigated in the frequency range 100 Hz to 15 MHz and in the temperature range from 300 K to above the glass transition temperature T_g. The frequency-dependent electrical data have been discussed in the framework of the complex impedance and the power-law conductivity. The electrical conductivity is strongly composition dependent and it follows the Arrhenius relation in the experimental temperature range. The activation energies of dc and ac conductivities obtained by the power-law analysis show that the BGSO glasses satisfy the Barton, Nakajima, and Namikawa (BNN) relation. The temperature-dependent interaction of conducting ions is discussed.

I. Introduction

Glasses containing heavy-metal oxide cations have been proposed as candidates for the scintillation detector because of their high stopping power and medical imagery that have long been known. Bismuth germanate $Bi_4Ge_3O_{12}$ (BGO) and bismuth silicate $Bi_4Si_3O_{12}$ (BSO) crystals are synthetic materials having a eulytite structure. These crystals are attractive because of their electrooptical,[1] electromechanical,[2] and intense luminescence properties, their short wavelength of radiation,[3] their laser materials when doped with rare earths, and the fact that they are nonhygroscopic. In particular, BGO has received a lot of attention because of its uses as a scintillator in X-ray and positron emission tomography, and in telescopes for hard X- and γ-rays in astrophysics and nuclear physics. Many studies on the ionic conductivity and relaxation in oxide glasses have been reported.[4−10] However, there has been a lack of a temperature-dependent dielectric study on the bismuth germanate silicate glasses.

In the present paper, we have studied the conductivity mechanism in $Bi_4(Ge_xSi_{1-x})_3O_{12}$ (BGSO) glasses at various temperatures, where $x = 0$, 0.33, 0.66, and 1. The complex impedance Cole−Cole plot and the power-law method[11−15] are adapted for the analysis of the electrical conductivities of dc and ac, and the BNN relation[16−18] is examined.

II. Experimental Section

Crystalline powders of $2Bi_2O_3-3[xGeO_2-(1-x)SiO_2]$, with $x = 0$, 0.33, 0.66, and 1 were well mixed and annealed for 20 h at 1123 K. The mixture was ground and the same annealing process was performed for 6 h. The powder samples were melted in a cylindrical electric furnace at 1423 K in air. The melted sample was quenched through a twin roller. The estimated cooling rate was about 10^5 K/s.

X-ray diffraction (XRD), differential scanning calorimetry (DSC), scanning electron microscopy (SEM), and Raman spectroscopy measurements were conducted to investigate the crystalline processes,[19] The glass transition temperature, T_g, and the crystallization temperature, T_c, were determined as the points where the DSC curves depart from the horizontal baselines and meet with an extrapolation at inflections of the thermal chord.

The electrical measurements, such as capacitance and conductance of the samples of thickness 0.1 mm and diameter ~8.8 mm, were carried out using an Impedance/Gain-Phase Analyzer (Hewlett-Packard LF4194A, United States) in the temperature range 300−923 K and in the frequency range 100 Hz−15 MHz, with the heating rate of 2 K/min. The parallel surfaces of the sample were coated by vacuum evaporation with gold for electrodes.

III. Results and Discussion

In this study, we simplify the notations according to the Ge/Si atomic ratio. They are $Bi_4Ge_3O_{12} \simeq$ BGO, $Bi_4Ge_2SiO_{12} \simeq$ BGSO(2:1), $Bi_4Ge_1Si_2O_{12} \simeq$ BGSO(1:2), $Bi_4Si_3O_{12} \simeq$ BSO, and $Bi_4(Ge_xSi_{1-x})_3O_{12} \simeq$ BGSO.

The as-quenched glass was measured by DSC to determine the glass transition temperature T_g and the supercooled liquid region. Figure 1(a) is the DSC curve for BGO glass, measured with a heating rate of 2 K/min. The glass-transition temperature is determined to be 700 K and the supercooled liquid region extends up to 760 K just before the start of crystallization appeared as an exothermic peak. Figure 1(b) is the complex impedance Cole−Cole plot of BGO glass for a few temperatures, measured with a heating rate of 2 K/min, and shows a typical depressed circular arc behavior. In Figure 1(b), the symbols are measured data and the lines are fitted with the Cole−Cole function

$$Z = \Delta R[1 + i(\omega\tau)^{\alpha}]^{-1} \quad (1)$$

where $\Delta R \simeq R_0 - R_\infty$, τ is the relaxation time, and α is the exponent related to the distribution of relaxation time.

The variation of the dc conductivity, calculated from the complex impedance Cole−Cole plots, with reciprocal temperature for various compositions of BGSO glasses is shown in

* Corresponding author. Tel: 82-51-510-2958. Fax: 82-51-516-5682. E-mail address: ysyang@pusan.ac.kr.

† Semyung University.

10.1021/jp040219q CCC: $27.50
Published on Web 10/02/2004

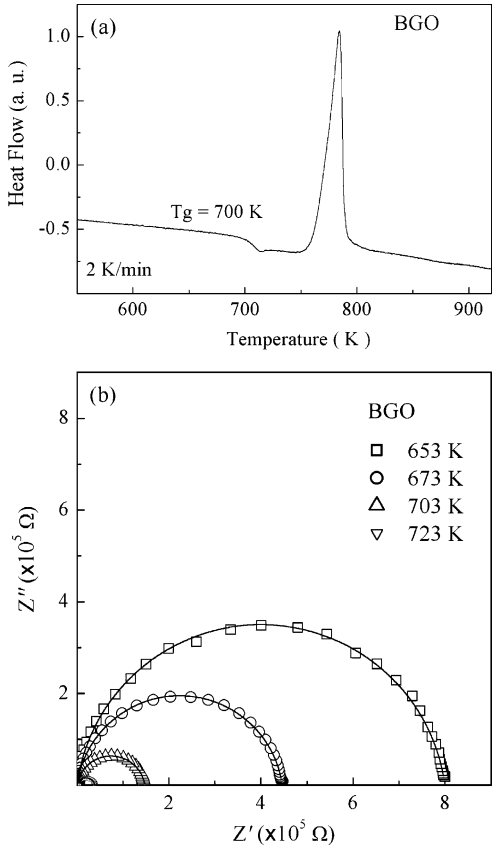

Figure 1. (a) DSC curve for BGO glass, measured with a heating rate of 2 K/min. (b) Complex impedance Cole−Cole plot of BGO glass for a few temperatures, measured with a heating rate of 2 K/min. The symbols are measured data and the lines are fit with the Cole−Cole function.

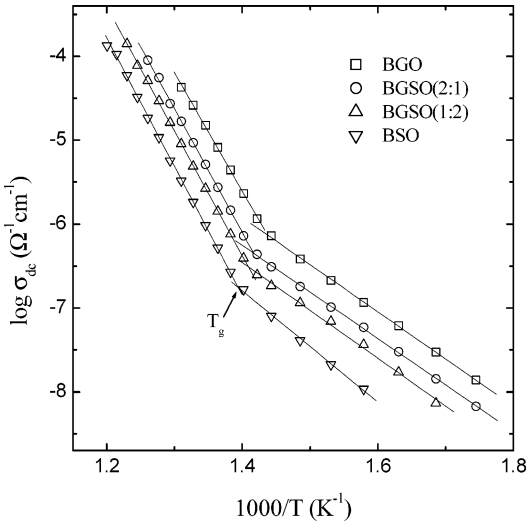

Figure 2. Temperature dependence of the dc conductivity for different compositions of BGSO glasses (shown) obtained from the fits of the complex impedance Cole−Cole analysis. The solid lines are the least-squares straight-line fits to the data.

Figure 2. The figure shows that the dc conductivity obeys the Arrhenius relation $\sigma_{dc} = C \exp(-E_{dc}/kT)$, where E_{dc} is the activation energy from the complex impedance plot and k is the Boltzmann constant. The slopes of least-squares straight-line fits represent the values of the activation energy for different compositions of BGSO glasses. The corresponding activation energies, E_{dc}, of the BGO, BGSO(2:1), BGSO(1:2), and BSO are 1.12, 1.09, 1.15, and 1.32 (eV) below T_g, and 2.80, 2.92, 2.95, and 3.04 (eV) above T_g, respectively. The activation energy increases, on the whole, with decreasing x. In the case of BGSO glasses, the glass-forming ability continues to increase with decreasing x.[19] The principal mobile cation is the Bi ion for BGSO in the network former such as SiO_2 and GeO_2; therefore, the dc conductivity and the activation energy for BGSO glass have been focused in the activity of the Bi.[20,21] As the Si content increases, the looseness of the structure of the glass network increases and there exists a high occupancy of nonbridging oxygen. Thus, the Bi cation can migrate with less ease relatively through the broken network. Correspondingly, dc conductivity decreases with increase in Si content, representing the higher activation energy.

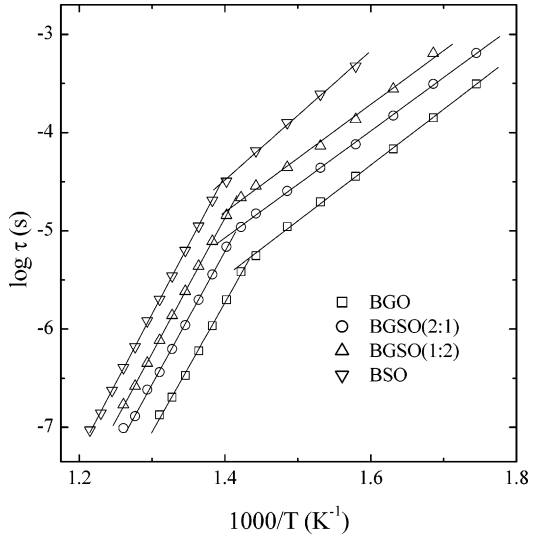

Figure 3. Temperature dependence of the conductivity relaxation times obtained from the complex impedance Cole−Cole analysis for different compositions of BGSO glasses shown. The solid lines represent the best fits with the Arrhenius relation $\tau = \tau_o \exp(E_{ac}/kT)$.

In Figure 3, we present the relaxation time τ, obtained from the impedance Cole−Cole plot as a function of 1000/T. The impedance plot shows typical arc behavior as shown in Figure 1. The peak frequency where the imaginary part of the complex impedance is a maximum, ω_p, that satisfies $\omega_p\tau = 1$.[22] The relaxation times with different slopes at T_g decrease as the temperature increases, indicating that the charge carrier moves back to an original state or locates at a stable energy state in a short time after an electrical impulse. The relaxation time also decreases with an increment of x, caused by an easy movement of the cation. The solid lines represent the best fits with the Arrhenius relation $\tau = \tau_o \exp(E_{ac}/kT)$. Correspondingly, the ac activation energies, E_{ac}, from the complex impedance plot for the BGO, BGSO(2:1), BGSO(1:2), and BSO are 1.11, 1.07, 1.10, and 1.30 (eV) below T_g, and 2.61, 2.62, 2.73, and 2.79 (eV) above T_g, respectively. The relaxation time increases rapidly at the glass transition temperature because of the structural relaxation in the supercooled state.

From the results of Figures 2 and 3, the corresponding activation energies for the dc conductivity, E_{dc}, are found to be slightly higher, above T_g, than those for the relaxation, E_{ac}, while E_{dc} are found to be close to E_{ac} below T_g.

We have studied the ac behavior of bismuth germanate silicate glass in the framework of the conductivity representation.[11−15] The frequency-dependent conductivity of ionic conducting glass can be interpreted as the result of ion movement through the ion matrix or ion−ion interaction.[23−26] Here, the principal mobile cation is the Bi ion for BGSO in the network former.

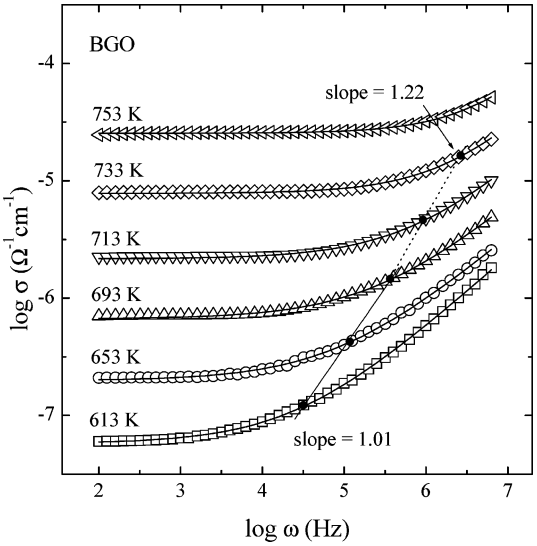

Figure 4. Frequency spectra of the real conductivity $\sigma(\omega)$ for BGO glass composition at several temperatures. The solid and dotted lines are obtained from a Jonscher's power-law fit of ac conductivities to eq 2. The slope represents the value of activation energy of the hopping frequency.

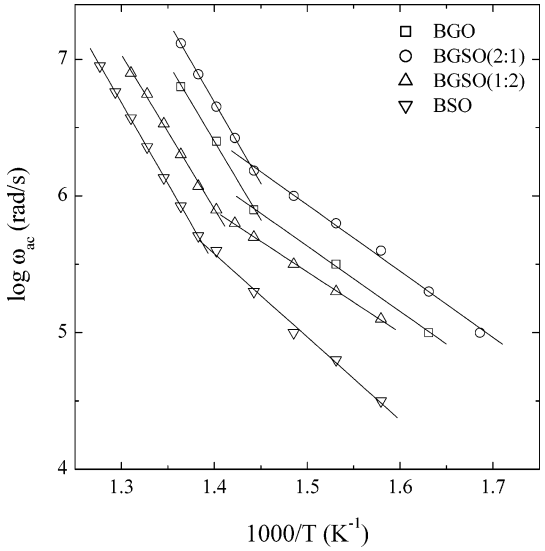

Figure 5. Reciprocal temperature dependence of hopping frequency for different compositions of BGSO glasses (shown) obtained from fit to $\sigma(\omega_{ac}) = 2\sigma'_{dc}$, The solid lines indicate that ω_{ac} obeys the Arrhenius relation.

In this formalism, the bulk frequency-dependent conductivity $\sigma(\omega)$ from the movement of dissociated cations in the glass matrix is described by

$$\sigma(\omega) = \sigma'_{dc} + A\omega^n = \sigma'_{dc}\,[1 + (\omega/\omega_{ac})^n] \qquad (2)$$

where σ'_{dc} is the dc conductivity from the power-law fit, A is a temperature-dependent parameter, ω_{ac} is the ionic hopping rate, and n is a frequency exponent parameter in the range $0 \le n \le 1$ characterizing the deviation from Debye behavior and measuring of the interionic coupling strength.[27−29]

At low frequencies, long-range diffusion of these cations results in the frequency-independent conduction σ'_{dc}. Here, the hopping frequency of the charge carriers ω_{ac} is related to the activation energy with a constant D. Moreover, the constant D involves an effective hopping frequency in the range $10^{10.5}$ to $10^{13.8}$ rad/s, which is close to the phonon frequency.[30] That is,

$$\omega_{ac} = D\exp(-E'_{ac}/kT) \qquad (3)$$

where E'_{ac} is the ac activation energy from the Jonscher's power law fit.

The frequency spectra of the real conductivity $\sigma(\omega)$ for a glass composition, BGO, is shown in Figure 4 at different temperatures. At lower frequencies, the conductivity is almost independent of frequency, approaching the dc conductivity in the plateau region. At higher frequencies, the conductivity shows a dispersion, which shifts to higher frequencies with increasing temperature. The experimental conductivity data for BGO have been fitted to eq 2, which is a Jonscher fit of ac conductivities. The best fits of the conductivity spectra at different temperatures are shown as solid lines in Figure 4. In the figure, we have the crossover frequency from the dc behavior to the dispersive conductivity, ω_{ac}, which increases with temperature. The corresponding crossover hopping frequency is connected by the relation as follows:

$$\log \sigma(\omega_{ac}) = \gamma \log \omega_{ac} \qquad (4)$$

where γ is the slope of each straight line in Figure 4.

The solid and dotted straight lines are obtained with slopes of 1.01 below T_g and of 1.22 above T_g.

The hopping rates are obtained from the conductivity spectrum in eq 2 by substitution ($\sigma(\omega_{ac}) = 2\sigma'_{dc}$), and the other parameters, A and n, by a linear least-squares fitting procedure. Here, the dc activation energies, σ'_{dc}, from the power-law fit in Figure 4 with the same process as shown in Figure 2 for the BGO, BGSO(2:1), BGSO(1:2), and BSO are 1.11, 1.15, 1.07, and 1.19 (eV) below T_g, and 3.01, 2.95, 2.91, and 2.95 (eV) above T_g, respectively.

From the data in Figure 3, we may obtain the characteristic peak frequency by the method of the complex impedance Cole−Cole plot, ω_p, for BGO by taking the inverse of τ at various temperatures. It can then be compared with the frequency obtained by the Jonscher's power-law method, ω_{ac}, represented as filled circles in Figure 4. The selected characteristic frequency, ω_p, is slightly low compared with ω_{ac}. The corresponding ac activation energies, despite the difference of the characteristic frequencies, are close to each other in the whole range of the experimental temperature. This implies that the energy barriers affecting the ac conductivity are not sensitive to the applied frequencies in the range of 10^4∼10^7 Hz.

The reciprocal temperature dependence of hopping frequency, ω_{ac}, is shown in Figure 5, which indicates that ω_{ac} obeys the Arrhenius relation. The value of the activation energy E'_{ac} of the hopping frequency obtained from the slopes of the BGO, BGSO (2:1), BGSO (1:2), and BSO are 1.04, 1.11, 0.85, and 1.06 (eV) below T_g and 2.42, 2.37, 2.25, and 2.34 (eV) above T_g, respectively.

Since eqs 3 and 4 can be rewritten as $\sigma(\omega_{ac}) \propto \omega_{ac}{}^{\gamma} \propto \exp(-\gamma E'_{ac}/kT)$ and $\sigma'_{dc} \propto \exp(-E'_{dc}/kT)$, we find the relation between the activation energy of the hopping frequency and the dc activation energy to be $E'_{dc} = 1.01E'_{ac}$ below T_g and $E'_{dc} = 1.22E'_{ac}$ above T_g, respectively. Correspondingly, the power-law dc activation energy of the hopping carriers, E'_{dc}, is close to the complex-impedance dc activation energy, E_{dc}, except for BGSO(1:2) and BSO below T_g.

This indicates that the BGSO glasses satisfy the BNN relation,[16−18] since the BNN relation implies $\omega_p \sim \sigma_{dc}$ or σ'_{dc} while σ_{dc}, σ'_{dc}, and ω_p are Arrhenius, and ω_p is the dielectric loss peak frequency.

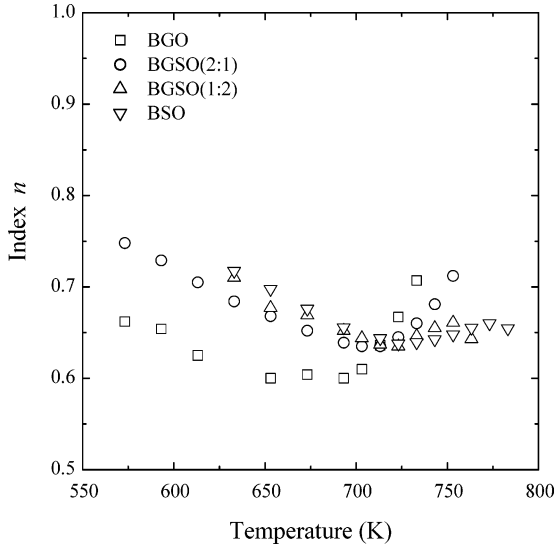

Figure 6. Temperature dependence of a frequency exponent parameter, which measures the interaction between mobile ions, for different compositions of BGSO glasses (shown) obtained from fit to eq 2.

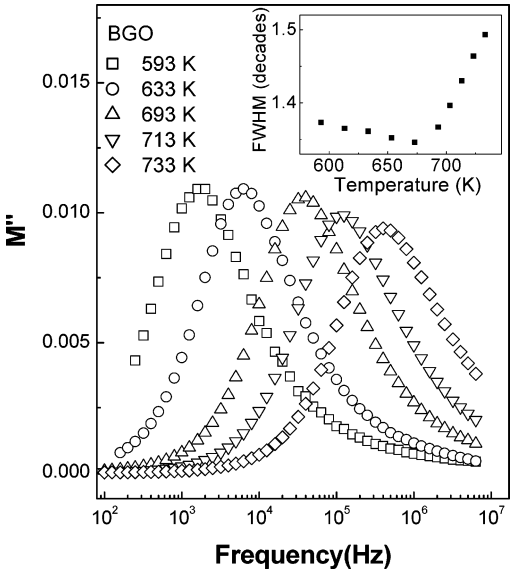

Figure 7. Frequency spectra of the imaginary part of the electric modulus for BGO glass at several temperatures. The inset shows the full width at half-maximum of $M''(w)$ versus temperature for BGO sample.

The tendencies of the conductivity variation with concentration and the exponent n with temperature are in basic agreement with the study of Monte Carlo simulations of a simple lattice−gas model by which the effect of both long-range Coulomb interactions between the mobile ions and structural disorder in the host lattice.[9,26]

The values of parameter n calculated from eq 2 in Figure 6 are decreasing with increasing temperature below T_g, but show an increasing trend with increasing germanium content above T_g. The temperature dependence of n is simply understood in that the looseness of the glass network increases with increasing temperature and the interactions between conducting ions and surrounding decrease below T_g (n being a measure of interaction). As we mentioned in Figure 2, stronger interaction of the cation in BSO is expected by the higher density of nonbridging oxygen from the loosened glass network, compared with that of BGO below T_g. In the supercooled liquid state, above T_g, a high value of n in BGO may be due to the fact that the chance for mobile ions to interact with other atoms increases with a pronounced decrease in viscosity. This phenomenon is partially understood from the previous thermal study work where the supercooled region of BGO is much narrower compared with the case of BSO, because a narrowness in temperature interval of supercooled state is a measure of structural instability.[19]

The electrical impedance data could also be analyzed by the electrical modulus representation of Macedo and Moynihan.[31−33] In Figure 7, we present an imaginary part of the electric modulus for BGO glass at various temperatures. Typical features exhibit a broad and asymmetric maximum peaked function of ω for $M''(\omega)$ whose frequency at maximum ω_m varies in proportion to the dc conductivity. The inset in Figure 7 shows the full width at half maximum (fwhm) of $M''(\omega)$ versus temperature for BGO sample. The fwhm was obtained by the best fit of the experimental curves. The fwhm for BGO glass is decreased below T_g but is increased with increasing temperature above T_g. This result is consistent with the one for the parameter n of the power-law representation shown in Figure 6.

IV. Conclusions

The complex impedance Cole−Cole and the power-law methods are adapted for the analysis of the electrical conductivities of BGSO glasses.

The dc conductivity decreases with increasing Si content because of the increase of interaction between Bi and nonbridging oxygen.

The composition-dependent activation energy increases with the decrease in compound of Ge over the whole range of the experimental temperature.

In the complex impedance analysis, the dc activation energy E_{dc} is found to be slightly higher than the ac activation energy for relaxation E_{ac} above T_g, while E_{dc} is found to be close to E_{ac} below T_g.

The power-law dc activation energy E'_{dc} of the hopping carrier is close to the complex impedance dc activation energy E_{dc} above T_g and for some compositions below T_g, which indicates that the BGSO glasses satisfy the BNN relation.

The values of parameter n decrease with increasing temperature below T_g, since the interaction of conducting ion in the glass matrix decreases due to the loosened network with temperature.

Acknowledgment. This research was supported by the Program for the Training of Graduate Students in Regional Innovation, which was conducted by the Ministry of Commerce, Industry and Energy of the Korean Government.

References and Notes

(1) Link, J.; Fontanella, J. *J. Appl. Phys.* **1980**, *51*, 4352.
(2) Schweppe, H. *IEEE Trans. Sonics Ultras.* **1969**, *SU-16*, 219.
(3) Moncorge, R.; Jacquier, B.; Boulon, G. *J. Lumin.* **1976**, *14*, 337.
(4) Angell, C. A. *Chem. Rev.* **1990**, *90*, 523.
(5) Elliott, S. R.; Owen, A. P. *Ber. Bunsen-Ges., Phys. Chem.* **1991**, *95*, 987.
(6) Bunde, A.; Ingram, M. D.; Maass, P. *J. Non-Cryst. Solids* **1994**, *172−174*, 1222.
(7) Sidebottom, D. L.; Green, P. F.; Brow, R. K. *J. Chem. Phys.* **1998**, *108*, 5870.
(8) Funke, K. *Prog. Solid State Chem.* **1993**, *22*, 111.
(9) Maass, P.; Meyer, M.; Bunde, A. *Phys. Rev. B* **1995**, *51*, 8164.
(10) Ngai, K. L. *J. Non-Cryst. Solids* **1996**, *103*, 232.
(11) Almond, D. P.; Duncan, G. K.; West, A. R. *Solid State Ionics* **1983**, *8*, 159; **1983**, *9*, 277.
(12) Nowick, A. S.; Lim, B. S. *J. Non-Cryst. Solids* **1994**, *172*, 1389.
(13) MacDonald, J. R. *J. Non-Cryst. Solids* **1996**, *197*, 83.
(14) Elliott, S. R. *J. Non-Cryst. Solids* **1994**, *170*, 97.
(15) Dyre, J. C. *J. Non-Cryst. Solids* **1991**, *135*, 219.

(16) Barton, J. L. *Verres Réfr.* **1996**, *20*, 328.
(17) Nakajima, T. In *1971 Annual Report, Conference on Electric Insulation and Dielectric Phenomena*; National Academy of Sciences: Washington, DC, 1972; p 168.
(18) Namikawa, H. *J. Non-Cryst. Solids* **1975**, *18*, 173.
(19) Cho, J. H.; Kim, S. J.; Yang, Y. S. *Solid State Commun.* **2001**, *119*, 465.
(20) Dumbaugh, W. H. *Phys. Chem. Glasses* **1978**, *19*, 121.
(21) Kusz, B.; Trzebiatowski, K.; Gazda, M.; Murawski, L. J. *J. Non-Cryst. Solids* **2003**, *328*, 137.
(22) Macdonald, J. R. *Impedance Spectroscopy*; John Wiley & Sons: New York, 1987; P. 14.
(23) Niklasson, G. A. *J. Appl. Phys.* **1987**, *62*, R1.
(24) Dissado, L. A.; Hill, R. M. *J. Appl. Phys.* **1987**, *66*, 2511.
(25) Sidebottom, D. L.; Green, P. F.; Brown, R. K. *Phys. Rev. B* **1995**, *51*, 2770.
(26) Maass, P.; Peterson, J.; Bunde, A.; Dieterich, W.; Roman, H. E. *Phys. Rev. Lett.* **1991**, *66*, 52.
(27) Ngai, K. L.; Rendell, R. W.; Jain, H. *Phys. Rev. B* **1984**, *30*, 2133.
(28) Ngai, K. L.; Mundy, J. N.; Jain, H.; Kannert, O.; Balzer-Jollenbeck, G. *Phys. Rev. B* **1989**, *39*, 6169.
(29) Kannert, O.; Steinert, J.; Jain, H.; Ngai, K. L. *J. Non-Cryst. Solids* **1991**, *131*, 1001.
(30) Beneventi, P.; Bersani, D.; Lottici, P. P.; Kovacs, L. *Solid State Commun.* **1995**, *93*, 143.
(31) Macedo, P. B.; Moynihan, C. T.; Bose, R. *Phys. Chem. Glasses* **1972**, *13*, 171.
(32) Howell, F. S.; Bose, R. A.; Macedo, P. B.; Moynihan, C. T. *J. Phys. Chem.* **1974**, *78*, 639.
(33) Hasz, W. C.; Moynihan, C. T.; Tick, P. A. *J. Non-Cryst. Solids* **1994**, *172*−*174*, 1363.